Exploring the effects of phase modulation on the dynamics of the kicked rotor systems

Mengyao Li, Yingying Xiao, Yongchun Tao, and Yi Gao*
Center for Quantum Transport and Thermal Energy Science, Jiangsu Key Lab on Opto-Electronic Technology, School of Physics and Technology, Nanjing Normal University, Nanjing 210023, China

Peiqing Tong†
School of Physics and Technology, Jiangsu Key Laboratory for Numerical Simulation of Large Scale Complex Systems, Nanjing Normal University, Nanjing 210023, China

(Received 14 December 2020; revised 10 October 2021; accepted 5 January 2022; published 20 January 2022)

Inspired by the recent experimental progress in the time-driven phase transition in quantum chaos, we investigate comprehensively the energy diffusion of a kicked rotor in the presence of phase modulation. In the classical case, we found that there always exists anomalous diffusion as long as the phase is modulated periodically and changes by 0 or π from kick to kick. On the contrary, for quasiperiodic and random phase modulation, anomalous diffusion is suppressed. On the other hand, in the quantum case, there exist only ballistic energy diffusion and dynamical localization in the standard and periodically shifted cases, while random phase modulation destroys the quantum coherence and totally suppresses the dynamical localization. Furthermore, the quasiperiodic phase modulation is an intermediate phase between the standard case and the random one. In both the classical and quantum cases, quasiperiodic phase modulation is inequivalent to random phase modulation at large kicking times ($>10^3$), thus caution has to be taken when dealing with these two kinds of phase modulation in experiments.

DOI: 10.1103/PhysRevE.105.014212

I. INTRODUCTION

The noise effect is of great significance to classical and quantum systems [1]. The properties of physical systems depend on the correlations between their degrees of freedom, and noise affects these correlations [2–4]. In particular, the dynamics of quantum systems is controlled by quantum interference [5–7], which is very sensitive to noise [8,9]. Subtle noise may destroy the correlations and drive the quantum system towards classical behavior [1,5,10]. Since the introduction of noise makes the quantum system in some sense more classical, it is ideal for studying quantum-classical correspondence [11]. Therefore, a research tool to accurately control the level of noise is required. The kicked rotor is one such tool [12], and it can be used to explore the effects of noise on classical and quantum systems.

The kicked rotor is a paradigm for studying classical and quantum chaos, since its model is very simple and it exhibits complex dynamics that can capture the essence of chaos [13–15]. In the field of classical chaos, the kicked rotor has been studied extensively as a fundamental nonlinear system, while from the perspective of quantum chaos the kicked rotor is easy to realize experimentally [11,16–18]. Although ballistic energy growth was not observed in the initial experiment [16] that meets the quantum resonance conditions, subsequent work [19] shows that this is due to insufficient experimental time, but not the system itself [11].

Modulation effects on kicked rotors have long been studied over the years, and they are often referred to as noise [1,5]. For example, previous studies have found that amplitude noise can suppress anomalous diffusion in the classical kicked rotor [20,21]. On the other hand, in quantum systems, by adding amplitude noise with new incommensurate frequencies, it has been proved that the kicked rotor is equivalent to the Anderson model, and it can be easily generalized to higher dimensions [14,22]. In three dimensions, the model demonstrates an effective metal-insulator transition [5,14,22]. Research also shows that, in quantum systems, the amplitude noise can destroy the dynamical localization, and it has no effect on quantum resonance [9,23], while the diffusion resonance is sensitive to the applied fluctuation of kicking strength [12]. Moreover, under the influence of quantum coherence, timing noise can destroy the dynamical localization and restore the energy diffusion [24], which has also been confirmed by experiments.

Spontaneous emission is also a kind of noise that affects coherence and dynamical behavior [18,25]. For example, spontaneous emission in a kicked rotor leads to a small increase in the momentum diffusion rate of the classical system [21] and a striking enhancement of the energy at resonance of the quantum system [5,11,26]. Furthermore, in a quantum kicked rotor, dynamical localization is a coherent effect, and the coupling between the system and the environment will affect it [8,10,25,27,28]. Thus, the introduction of decoherence into the quantum kicked rotor by spontaneous emission destroys the original coherence, thus

*flygaoonly@njnu.edu.cn
†pqtong@njnu.edu.cn

destroying the dynamical localization and leading to quantum diffusion [18,25,28].

Furthermore, the noise on the kicking frequency destroys the dynamical localization in the quantum system [12], while preliminary research shows that quantum resonance is robust against certain types of phase noise [5]. Precise phase modulation of an optical potential can be achieved experimentally, which allows researchers to control the quantum correlations. Therefore, relevant experiments have attracted much attention [29,30].

In this paper, we study comprehensively the effects of phase modulation on the dynamical behavior of classical and quantum kicked rotors. We found that different types and strengths of phase modulation may lead to various dynamical behaviors, some of which are quite distinct from those previously studied.

II. METHOD

We consider a kicked rotor whose Hamiltonian is given by [5,29,30]

$$H(t) = \frac{L^2}{2m} + K\cos[\theta - a(t)]\sum_n \delta(t - nT), \tag{1}$$

where L is the angular momentum, m is the mass, n is an integer, T is the kicking period, K is the kicking strength, θ is the angular position (for example, on a ring), taken modulo 2π, $a(t)$ is the phase, and δ is the Dirac delta function. Furthermore, the initial state is started at $t = 0^-$. For simplicity, we omit the superscript $-$ in t throughout this work.

For the classical kicked rotor, the dynamics of the system can be described by the standard map,

$$\begin{aligned} L_{n+1} &= L_n + K\sin(\theta_n - a_n), \\ \theta_{n+1} &= \theta_n + \frac{T}{m}L_{n+1}, \end{aligned} \tag{2}$$

where the subscript n represents the quantities at $t = nT$.

On the other hand, for the quantum kicked rotor, the dynamics of the system is determined by the Schrödinger equation

$$i\hbar\frac{\partial\Psi(\theta,t)}{\partial t} = H(t)\Psi(\theta,t), \tag{3}$$

and the time evolution operator over one period can be written as [5]

$$U(n+1,n) = e^{-i\frac{L^2T}{2m\hbar}}e^{-i\frac{K}{\hbar}\cos(\theta-a_n)}, \tag{4}$$

which relates the wave functions at $t = nT$ and $t = (n+1)T$ as

$$\Psi[\theta,(n+1)T] = U(n+1,n)\Psi(\theta,nT). \tag{5}$$

Here, L should be replaced by $-i\hbar\frac{\partial}{\partial\theta}$, and $\hbar$ is the reduced Planck constant [31].

The wave function $\Psi(\theta,t)$ can be expressed by Fourier transform as $\Psi(\theta,t) = \sum_l e^{il\theta}\psi_l(t)$, and since $Le^{il\theta} = \hbar l e^{il\theta}$ [32], we have the iteration relation

$$\psi_{l'}[(n+1)T] = e^{-i\frac{\hbar T}{2m}l'^2}\sum_l J_{l-l'}\left(-\frac{K}{\hbar}\right)i^{l-l'}e^{i(l-l')a_n}\psi_l(nT), \tag{6}$$

where

$$J_{l-l'}\left(-\frac{K}{\hbar}\right) = \frac{1}{2\pi}i^{-(l-l')}\int_0^{2\pi} d\theta\, e^{i(l-l')\theta}e^{-i\frac{K}{\hbar}\cos\theta}. \tag{7}$$

Here $J_{l-l'}(-\frac{K}{\hbar})$ is the Bessel function of the first kind. In the numerical calculation, the value of l in Eq. (6) is from $-M+1$ to M, and we set $M = 5\times10^5$. At every step of the iteration, we calculate the probabilities of particles appearing at the boundary of momentum space (i.e., $|\psi_M|^2$ and $|\psi_{-M+1}|^2$), and they are always less than 10^{-20}. Therefore, we believe that the grid is sufficiently large, and all the components do not run over the boundary of momentum space.

The energy diffusion is very helpful in understanding the dynamical behavior of the kicked rotor, therefore in this work, we study the expectation value of the rotor's energy growth, which is defined as

$$\langle\Delta L^2(t)\rangle = \langle L^2(t) - L^2(0)\rangle. \tag{8}$$

In the classical system, we average over various initial conditions to calculate $\langle\Delta L^2(t)\rangle$. In the quantum system, we set the initial state to be $\Psi(\theta,0) = \frac{1}{\sqrt{2\pi}}$ at $t = 0$, i.e., $\psi_l(0) = \frac{1}{\sqrt{2\pi}}\delta_{l,0}$. Throughout this work, we concentrate only on those times that are integer multiples of the kicking period, i.e., $t = nT$.

III. RESULTS AND DISCUSSION

We consider five types of phase modulation in the kicked rotor system.

(i) The standard kicked rotor where $a(t)$ is constant. This model has been studied for many years.

(ii) The periodically shifted kicked rotor with $a(t) = a(t + PT)$, where P is an integer and $P \neq 1$. To be specific, we set $a(t) = \pi\cos(2\pi v\frac{t}{T})$ with $v = 0.25$ (therefore, $P = 4$). In this case, the phase $a(t)$ is periodically modulated with a sinusoidal form, and it jumps by π from kick to kick [5].

(iii) Another type of periodically shifted kicked rotor, where we also set $P = 4$ and average over 100 sets of $\{a_0, a_1, a_2, a_3\}$ picked randomly from $-\pi$ to π [29].

(iv) The randomly shifted kicked rotor where each $a(t)$ is randomly distributed from $-\pi$ to π. In this case, the results presented below have also been averaged over 100 different realizations. We adopt this type of phase modulation in order to study the effect of uncorrelated phase modulation on the dynamical properties of the system.

(v) The quasiperiodically shifted kicked rotor, where we set $a(t) = \pi\cos(2\pi v\frac{t}{T})$ with $v = \frac{\sqrt{5}-1}{2}$, which is considered to be, in some sense, the most irrational number. In this case, the frequency of the phase modulation is incommensurate with respect to the kicking frequency [5].

The rotor's energy growth $\langle\Delta L^2(t)\rangle$ at large t can be generally expressed as

$$\langle\Delta L^2(t)\rangle \sim t^\alpha, \tag{9}$$

and since we consider only $t = nT$, we have [33]

$$\langle\Delta L_n^2\rangle \sim n^\alpha. \tag{10}$$

In the following, we use this relation to analyze the dynamical behaviors of the kicked rotor.

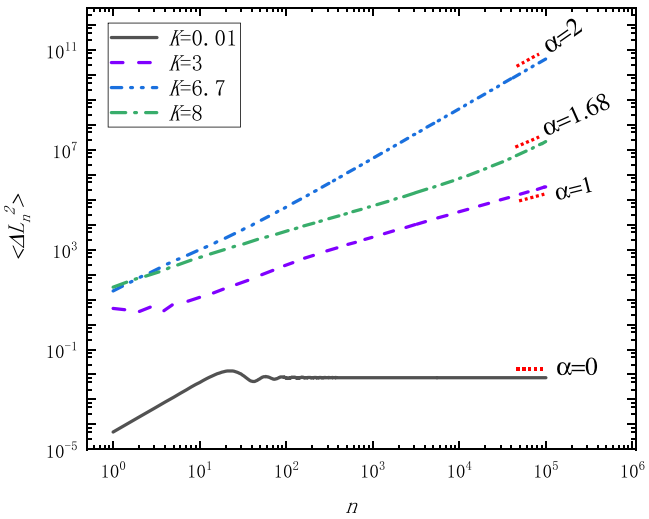

FIG. 1. Log-log plot of the expectation value of the rotor's energy growth $\langle \Delta L_n^2 \rangle$ in the standard kicked rotor, for the classical case. Both the phase $a(t)$ and the initial angular momentum L_0 are set to 0. For the initial angular position, we use 10^5 values of θ_0 evenly spaced between $-\pi$ and π. In addition, we also include those θ_0 satisfying $\frac{T}{m}K \sin\theta_0 = \pm 2\pi$ and $\theta_0 \in [-\pi, \pi]$. Here we set $T = 1$ and $m = 1$. $\langle \Delta L_n^2 \rangle$ is then calculated by averaging over all these θ_0. The red dotted line is a guide to the eye, showing the diffusion index α by fitting the data between $5 \times 10^4 \leqslant n \leqslant 10^5$ to Eq. (10).

A. Classical kicked rotor

The dynamics of the classical kicked rotor is determined by Eq. (2), and we have [33]

$$L_n = L_0 + K \sum_{i=0}^{n-1} \sin(\theta_i - a_i),$$

$$L_n^2 = L_0^2 + 2L_0 K \sum_{i=0}^{n-1} \sin(\theta_i - a_i) + K^2 \sum_{i,j=0}^{n-1} \sin(\theta_i - a_i)\sin(\theta_j - a_j), \tag{11}$$

and

$$\begin{aligned}\Delta L_n^2 &= L_n^2 - L_0^2 \\ &= 2L_0 K \sum_{i=0}^{n-1} \sin(\theta_i - a_i) \\ &\quad + K^2 \sum_{i,j=0}^{n-1} \sin(\theta_i - a_i)\sin(\theta_j - a_j) \\ &= 2L_0 K \sum_{i=0}^{n-1} \sin(\theta_i - a_i) + K^2 \sum_{i=0}^{n-1} \sin^2(\theta_i - a_i) \\ &\quad + K^2 \sum_{i,j=0, i\neq j}^{n-1} \sin(\theta_i - a_i)\sin(\theta_j - a_j).\end{aligned} \tag{12}$$

For the standard kicked rotor, if $\frac{T}{m}L_0 = 2k\pi$ and $\frac{T}{m}K \sin(\theta_0 - a_0) = 2l\pi$ [33], then it can be verified that

$$\Delta L_n^2 = K \sin(\theta_0 - a_0)[K \sin(\theta_0 - a_0)n^2 + 2L_0 n]. \tag{13}$$

Therefore, along this special class of trajectories in the (L, θ) phase space, if $K \sin(\theta_0 - a_0) \neq 0$, the rotor's energy growth will show an n^2 dependence [if $K \sin(\theta_0 - a_0) = 0$, the rotor's energy will not vary with n], which we denote as resonance [33]. On the contrary, if $\frac{T}{m}L_0 = (2k+1)\pi$ and $\frac{T}{m}K \sin(\theta_0 - a_0) = 2l\pi$, then we will have $L_n = L_0$ (for even n) and $L_n = L_0 + K \sin(\theta_0 - a_0)$ (for odd n). In this case, ΔL_n^2 will oscillate between 0 and $K \sin(\theta_0 - a_0)[K \sin(\theta_0 - a_0) + 2L_0]$. Therefore, we denote this case as antiresonance. Similarly, if $\frac{T}{m}L_0 = 2k\pi$ and $\frac{T}{m}K \sin(\theta_0 - a_0) = (2l+1)\pi$, then it can be proved that

$$\Delta L_n^2 = \begin{cases} 0 \quad \text{for even } n, \\ K \sin(\theta_0 - a_0)[K \sin(\theta_0 - a_0) + 2L_0] & \text{when } \mathrm{mod}(n, 4) = 1, \\ K \sin(\theta_0 - a_0)[K \sin(\theta_0 - a_0) - 2L_0] & \text{when } \mathrm{mod}(n, 4) = 3. \end{cases} \tag{14}$$

Furthermore, if $\frac{T}{m}L_0 = (2k+1)\pi$ and $\frac{T}{m}K \sin(\theta_0 - a_0) = (2l+1)\pi$, then

$$\Delta L_n^2 = \begin{cases} 0 \quad \text{when } \mathrm{mod}(n, 4) = 0, \\ K \sin(\theta_0 - a_0)[K \sin(\theta_0 - a_0) + 2L_0] & \text{when } \mathrm{mod}(n, 4) = 1 \text{ or } 3, \\ 4K \sin(\theta_0 - a_0)[K \sin(\theta_0 - a_0) + L_0] & \text{when } \mathrm{mod}(n, 4) = 2. \end{cases} \tag{15}$$

Since ΔL_n^2 in Eqs. (14) and (15) also oscillates around a fixed value periodically, we denote the initial conditions that led to Eqs. (14) and (15) as antiresonance as well. As long as the resonance is included in the initial conditions we choose, then the expectation value of the rotor's energy growth $\langle \Delta L_n^2 \rangle$ will exhibit anomalous diffusion at large n [$1 < \alpha \leqslant 2$ in Eq. (10)]. As can be seen from Fig. 1, for small enough $\frac{T}{m}K$ ($K = 0.01$), the diffusion index α is 0. For larger values of $\frac{T}{m}K$ satisfying $|\frac{T}{m}K| < 2\pi$ ($K = 3$), we have $\alpha = 1$ (normal diffusion). For $|\frac{T}{m}K| > 2\pi$ ($K = 6.7$ and 8), anomalous diffusion shows up, which is signified by $1 < \alpha \leqslant 2$.

In Fig. 2, we show the θ-L phase map of the standard map with different initial conditions. In the $K = 0.01$ case, a particle returns to its original point after N iterations, and all the trajectories look regular [see Fig. 2(a)] and they lead to localization. Furthermore, we also observe the growth of the chaotic region with increasing K. Thus, in the $K = 3$ case, the regular regions shrink into two blank areas and the chaotic

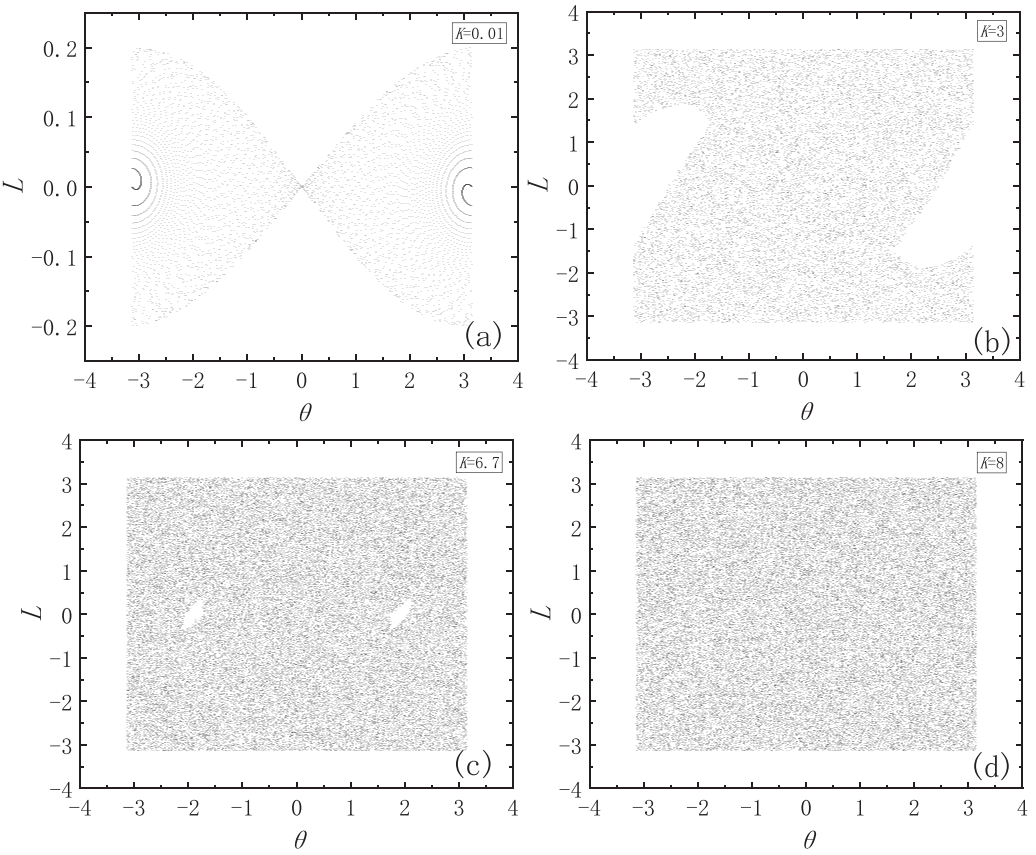

FIG. 2. The θ (mod 2π) and L (mod 2π) phase space of the standard map. For the initial angular position, we use 10^5 values of θ_0 evenly spaced between $-\pi$ and π, and the initial angular momentum L_0 is set to 0. Part (a) shows trajectories for the $K = 0.01$ case, corresponding to the regular regions. Part (b) shows trajectories for the $K = 3$ case, corresponding to the mixed regions (chaos and regular orbits). Part (c) shows trajectories for the $K = 6.7$ case, where the islands correspond to the accelerator mode. Part (d) shows trajectories for the $K = 8$ case, corresponding to the chaotic regions, and the accelerator island shrinks to a point in the phase space.

regions occupy most dark areas, and the dynamical behavior is mixed [chaos and regular orbits; see Fig. 2(b)] and leads to normal diffusion. Later, accelerator modes can be found around each of the stable accelerating fixed points (e.g., $K = 6.7$). In the $K = 6.7$ case, around the accelerator mode, the particle does not return to its original point after N iterations, but instead goes to the island that is shifted up or down by some multiple of 2π in L and causes ballistic diffusion. We can see that the accelerator modes exist only in a small region of phase space [see the small islands in Fig. 2(c)]. Finally, for the $K = 8$ case, at first glance, the chaotic sea extends over all phase space, which should lead to normal diffusion. However, it has an accelerator mode when θ_0 meets the resonance condition, and the accelerator island shrinks to a point in the phase space. Therefore in this case, if the accelerator mode is added, then the energy will show anomalous diffusion. In the other four cases with the addition of phase modulation, the energy diffusion can be similarly linked to Fig. 2. Previously, Ref. [33] studied the same standard kicked rotor, but found that the anomalous diffusion is restricted inside some specific K intervals (see Fig. 2 of Ref. [33]). The differences between Ref. [33] and ours can be understood as follows. In Ref. [33], it calculated $\langle \Delta L_n^2 \rangle$ by using 10^4 values of θ_0 evenly spaced between 0 and 2π. In this case, only a few θ_0 can satisfy the resonance condition, while most θ_0 cannot. Suppose, ideally, for those θ_0 that satisfy the resonance condition, $\Delta L_n^2 \propto n^2$, and for those that do not, $\Delta L_n^2 \propto n$. If we further assume that the portion of θ_0 satisfying the resonance condition is y, then we will have $\langle \Delta L_n^2 \rangle = yn^2 + (1 - y)n$. Next, Ref. [33] extracted the value of α by fitting from $n = 1000$ to 5000 kicks. In this case, only in some specific K intervals can yn^2 be comparable to, or larger than, $(1 - y)n$, i.e., anomalous diffusion. However, theoretically speaking, if $n \to \infty$, then $\langle \Delta L_n^2 \rangle$ will show an n^2 dependence as long as y is not exactly 0. Therefore in our work, in addition to 10^5 values of θ_0 evenly spaced between 0 and 2π, we further include four special θ_0 that satisfy $K \sin \theta_0 = \pm 2\pi$ (see the caption of Fig. 1). In this way, y is increased. Furthermore, we fit the data from $n = 5 \times 10^4$ to 10^5, which is closer to the $n \to \infty$ condition. Thus in our work, we conclude that the anomalous diffusion will show up as long as the resonance condition is included in calculating $\langle \Delta L_n^2 \rangle$. Finally we notice, in Fig. 1, for $n = 1000$ to 5000, the green curve ($K = 8$) almost has the same slope as the violet one ($K = 3$), therefore if we only fit to this interval, the anomalous diffusion in the $K = 8$ case will be missed.

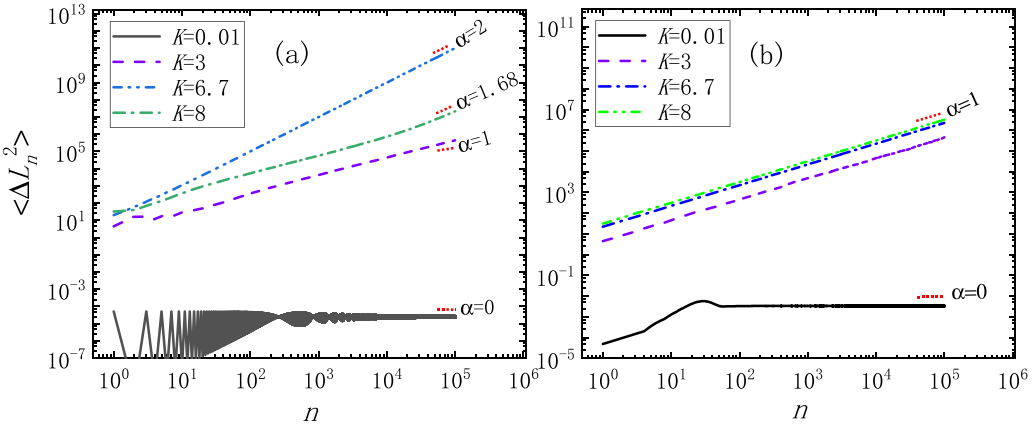

FIG. 3. Similar to Fig. 1, but for the periodically shifted case with $a_n = \pi \cos(\frac{\pi}{2}n)$ [see (a)] and $\{a_0, a_1, a_2, a_3\}$ picked randomly from $-\pi$ to π [see (b)]. For the initial conditions, we set $L_0 = 0$ and take 10^5 values of θ_0 evenly spaced between $-\pi$ and π. For (a), we also include the initial conditions $\frac{T}{m}L_0 = \pi$ and $\frac{T}{m}K\sin(\theta_0 - a_0) = \pm 2\pi$ ($\theta_0 \in [-\pi, \pi]$). For (b), an additional average over 100 sets of random numbers is implemented. Here we still set $T = 1$ and $m = 1$. $\langle \Delta L_n^2 \rangle$ is then calculated by averaging over all these L_0 and θ_0.

Similarly, for the periodically shifted case with $a_n = \pi\cos(\frac{\pi}{2}n)$, the phase a_n changes by π from kick to kick and we can prove that the resonance condition now becomes $\frac{T}{m}L_0 = (2k+1)\pi$ and $\frac{T}{m}K\sin(\theta_0 - a_0) = 2l\pi$. In this case,

$$\Delta L_n^2 = K\sin(\theta_0 - a_0)[K\sin(\theta_0 - a_0)n^2 + 2L_0 n]. \tag{16}$$

On the contrary, for $\frac{T}{m}L_0 = 2k\pi$ and $\frac{T}{m}K\sin(\theta_0 - a_0) = 2l\pi$,

$$\Delta L_n^2 = \begin{cases} 0 & \text{for even } n, \\ K\sin(\theta_0 - a_0)[K\sin(\theta_0 - a_0) + 2L_0] & \text{for odd } n. \end{cases} \tag{17}$$

For $\frac{T}{m}L_0 = 2k\pi$ and $\frac{T}{m}K\sin(\theta_0 - a_0) = (2l+1)\pi$,

$$\Delta L_n^2 = \begin{cases} 0 & \text{when } \mathrm{mod}(n,4) = 0, \\ K\sin(\theta_0 - a_0)[K\sin(\theta_0 - a_0) + 2L_0] & \text{when } \mathrm{mod}(n,4) = 1 \text{ or } 3, \\ 4K\sin(\theta_0 - a_0)[K\sin(\theta_0 - a_0) + L_0] & \text{when } \mathrm{mod}(n,4) = 2. \end{cases} \tag{18}$$

And for $\frac{T}{m}L_0 = (2k+1)\pi$ and $\frac{T}{m}K\sin(\theta_0 - a_0) = (2l+1)\pi$,

$$\Delta L_n^2 = \begin{cases} 0 & \text{for even } n, \\ K\sin(\theta_0 - a_0)[K\sin(\theta_0 - a_0) + 2L_0] & \text{when } \mathrm{mod}(n,4) = 1, \\ K\sin(\theta_0 - a_0)[K\sin(\theta_0 - a_0) - 2L_0] & \text{when } \mathrm{mod}(n,4) = 3. \end{cases} \tag{19}$$

Therefore, the initial conditions that lead to Eqs. (17)–(19) are now the antiresonance conditions in this periodically shifted case. As long as the resonance is included in the initial conditions, $\langle \Delta L_n^2 \rangle$ in this periodically shifted case will also exhibit anomalous diffusion at large n, similar to the standard case, as can be seen from Fig. 3(a). If we decrease the strength of the phase modulation, for example if we set $a_n = \frac{\pi}{6}\cos(\frac{\pi}{2}n)$, then the phase a_n will change by $\frac{\pi}{6}$ from kick to kick, instead of π, thus the previous resonance condition is not applicable. In this case, the energy growth only shows localization and normal diffusion, as shown in Fig. 4(a).

For the other periodically shifted case with $\{a_0, a_1, a_2, a_3\}$ picked randomly from $-\pi$ to π, in Eq. (12), after averaging over various initial conditions and 100 sets of random number realizations, we have $\langle \sin(\theta_i - a_i)\rangle = 0$, $\langle \sin^2(\theta_i - a_i)\rangle = \frac{1}{2}$, and $\langle \sin(\theta_i - a_i)\sin(\theta_j - a_j)\rangle = 0$ (for $i - j \neq 4k$). $\langle \cdots \rangle$ denotes the ensemble average, which means that θ_0 is averaged 10^5 times and a_n is averaged 100 times. On the other hand, for $i - j = 4k$ with $k \neq 0$, it can be proved that $\langle \sin(\theta_i - a_i)\sin(\theta_j - a_j)\rangle \neq 0$, and if we assume full correlation between θ_i and θ_j in this case, i.e., $\theta_i = \theta_j + 2l\pi$, then the upper

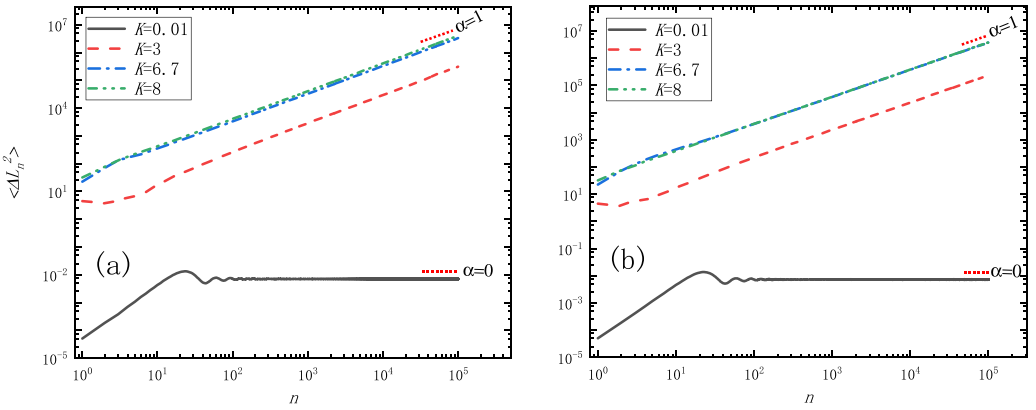

FIG. 4. (a) Similar to Fig. 3(a), but for the periodically shifted case with $a_n = \frac{\pi}{6}\cos(\frac{\pi}{2}n)$. (b) Similar to Fig. 3(b), but for periodically shifted case with $\{a_0, a_1, a_2, a_3\}$ picked randomly from $-\frac{\pi}{6}$ to $\frac{\pi}{6}$.

bound of Eq. (12) can be obtained as

$$\begin{aligned}
&\langle \Delta L_n^2 \rangle = \frac{K^2}{2} n \quad \text{for } 1 \leqslant n \leqslant 4, \\
&\langle \Delta L_n^2 \rangle \leqslant \frac{K^2}{2} n + \frac{K^2}{8} n(n-4) \quad \text{for } n > 4 \text{ and } \mathrm{mod}(n,4) = 0, \\
&\langle \Delta L_n^2 \rangle \leqslant \frac{K^2}{2} n + \frac{K^2}{8} (n-1)(n-3) \quad \text{for } n > 4 \text{ and } \mathrm{mod}(n,4) = 1 \text{ or } 3, \\
&\langle \Delta L_n^2 \rangle \leqslant \frac{K^2}{2} n + \frac{K^2}{8} (n-2)^2 \quad \text{for } n > 4 \text{ and } \mathrm{mod}(n,4) = 2.
\end{aligned} \tag{20}$$

As can be seen from Fig. 3(b), when K is small (e.g., $K = 0.01$), the expectation value of the rotor's energy saturates at large n [$\alpha = 0$ in Eq. (10)], while when K is larger, $\langle \Delta L_n^2 \rangle$ shows normal diffusion. Therefore, there exists a localization-delocalization transition in this case. And if $\{a_0, a_1, a_2, a_3\}$ is picked randomly from $-\frac{\pi}{6}$ to $\frac{\pi}{6}$, the conclusion is qualitatively similar, as shown in Fig. 4(b).

For the randomly shifted case, since each a_n in Eq. (12) is randomly distributed from $-\pi$ to π, we have $\langle \sin(\theta_i - a_i) \rangle = 0$, $\langle \sin^2(\theta_i - a_i) \rangle = \frac{1}{2}$, and $\langle \sin(\theta_i - a_i) \sin(\theta_j - a_j) \rangle = 0$ (for $i \neq j$). The ensemble-averaged result is $\langle \Delta L_n^2 \rangle = \frac{K^2}{2} n$, which means that in this case, the expectation value of the rotor's energy growth always shows normal diffusion [$\alpha = 1$ in Eq. (10)], as long as $K \neq 0$, as shown in Fig. 5(a). When each a_n in Eq. (12) is randomly distributed from $-\frac{\pi}{6}$ to $\frac{\pi}{6}$, the energy growth still shows normal diffusion and the conclusion is qualitatively similar to the case above at large n, as shown in Fig. 6(a).

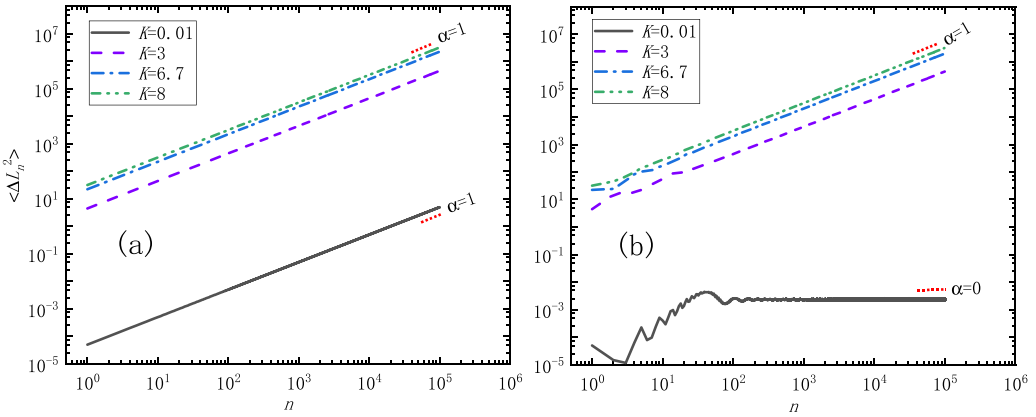

FIG. 5. (a) $\langle \Delta L_n^2 \rangle$ in the randomly shifted kicked rotor, which is calculated by the same averaging procedure as adopted in Fig. 3(b). (b) Similar to (a), but for the quasiperiodically shifted case. We generate a very long quasiperiodic sequence according to $a_n = \pi \cos[(\sqrt{5} - 1)n\pi]$, and $\langle \Delta L_n^2 \rangle$ is further averaged over 100 sets of quasiperiodic number realizations. The parameters T and m, as well as the initial conditions L_0 and θ_0, are all taken to be the same as those in Fig. 3(b).

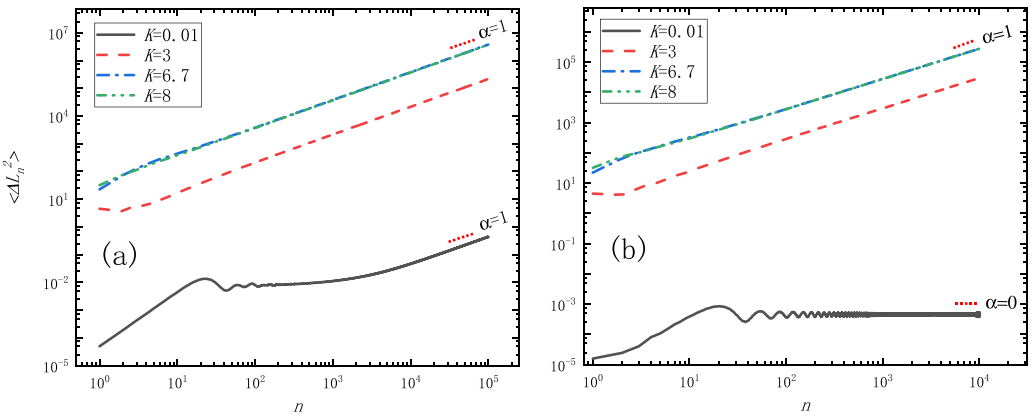

FIG. 6. (a) Similar to Fig. 5(a), but for the randomly shifted case with each a_n randomly distributed from $-\frac{\pi}{6}$ to $\frac{\pi}{6}$. (b) Similar to Fig. 5(b), but for the quasiperiodically shifted case with $a_n = \frac{\pi}{6}\cos[\pi(\sqrt{5}-1)n]$.

Finally, for the quasiperiodically shifted case, although the phase a_n seems to form a pseudorandom sequence, its dynamical behavior is different from that of the randomly shifted case. Specifically, for $K < K_c$ (e.g., $K = 0.01$), the expectation value of the rotor's energy saturates at large n [$\alpha = 0$ in Eq. (10)], while above K_c, $\langle \Delta L_n^2 \rangle$ shows normal diffusion, as shown in Fig. 5(b). Here K_c refers to the critical value of the kicking strength when the energy growth changes from localization to delocalization. Therefore, there exists a localization-delocalization transition in this quasiperiodically shifted case, as opposed to the randomly shifted one. And if we set $a_n = \frac{\pi}{6}\cos[\pi(\sqrt{5}-1)n]$, the result is similar to the above case, as shown in Fig. 6(b).

In short, in the classical kicked rotor with phase modulation, anomalous diffusion is a common phenomenon as long as the phase a_n is periodically modulated and changes by 0 or π from kick to kick. On the contrary, for the random and quasiperiodic phase modulation, the anomalous diffusion is suppressed, and the effect of quasiperiodic phase modulation is inequivalent to the random one when $n \geqslant 10^2$.

B. Quantum kicked rotor

We solve the Schrödinger equation for the kicked rotor in a quantum system, and we obtain an analytical formula for the momentum diffusion [34]. Then we use numerical simulation to verify the analytical solutions of quantum resonance and antiresonance.

Since we assume $\psi_l(0) = \frac{1}{\sqrt{2\pi}}\delta_{l,0}$, from Eq. (6) we have

$$
\begin{aligned}
\psi_{l_1}(T) &= \frac{1}{\sqrt{2\pi}} e^{-i\frac{\hbar T}{2m}l_1^2} i^{-l_1} e^{-il_1 a_0} J_{-l_1}\left(-\frac{K}{\hbar}\right),\\
\psi_{l_n}(nT) &= \frac{1}{\sqrt{2\pi}} e^{-i\frac{\hbar T}{2m}l_n^2} i^{-l_n} e^{-il_n a_{n-1}}\\
&\quad\times \sum_{l_{n-1}} e^{il_{n-1}(a_{n-1}-a_{n-2})} e^{-i\frac{\hbar T}{2m}l_{n-1}^2} J_{l_{n-1}-l_n}\left(-\frac{K}{\hbar}\right)\\
&\quad\vdots\\
&\quad\times \sum_{l_1} e^{il_1(a_1-a_0)} e^{-i\frac{\hbar T}{2m}l_1^2} J_{l_1-l_2}\left(-\frac{K}{\hbar}\right) J_{-l_1}\left(-\frac{K}{\hbar}\right) \quad \text{for } n \geqslant 2
\end{aligned}
\tag{21}
$$

and

$$
\begin{aligned}
|\psi_{l_1}(T)|^2 &= \frac{1}{2\pi} J_{-l_1}^2\left(-\frac{K}{\hbar}\right),\\
|\psi_{l_n}(nT)|^2 &= \frac{1}{2\pi}\sum_{l_1}\cdots\sum_{l_{n-1}}\sum_{l_1'}\cdots\sum_{l_{n-1}'} e^{i\frac{\hbar T}{2m}(l_{n-1}'^2-l_{n-1}^2)}\cdots e^{i\frac{\hbar T}{2m}(l_1'^2-l_1^2)} e^{i(l_{n-1}-l_{n-1}')(a_{n-1}-a_{n-2})}\cdots e^{i(l_1-l_1')(a_1-a_0)}\\
&\quad\times J_{l_{n-1}-l_n}\left(-\frac{K}{\hbar}\right)\cdots J_{l_1-l_2}\left(-\frac{K}{\hbar}\right) J_{-l_1}\left(-\frac{K}{\hbar}\right) J_{l_{n-1}'-l_n}\left(-\frac{K}{\hbar}\right)\cdots J_{l_1'-l_2'}\left(-\frac{K}{\hbar}\right) J_{-l_1'}\left(-\frac{K}{\hbar}\right) \quad \text{for } n \geqslant 2.
\end{aligned}
\tag{22}
$$

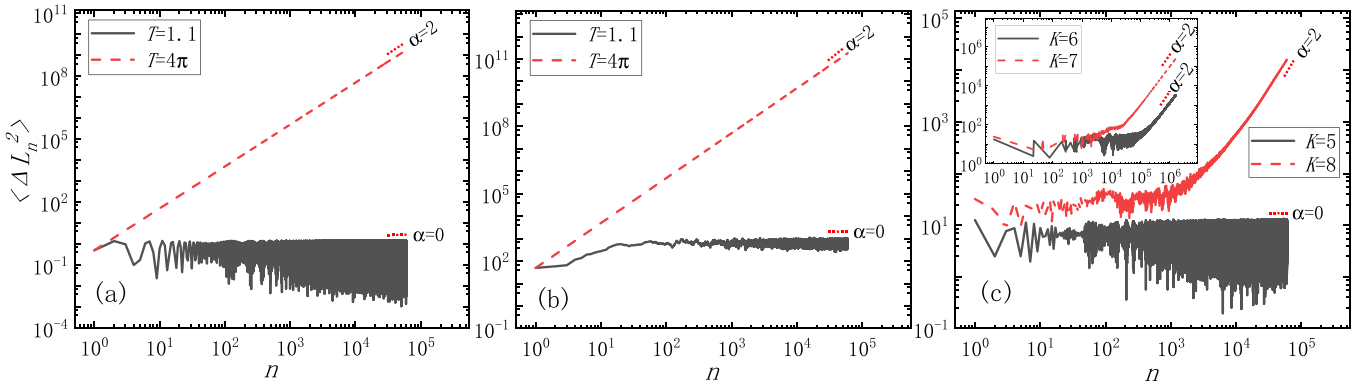

FIG. 7. Log-log plot of the expectation value of the rotor's energy growth $\langle \Delta L_n^2 \rangle$ in the standard kicked rotor for the quantum case. The parameters are chosen to be $\hbar = 1$, $m = 1$. The red dotted line is a guide to the eye, showing the diffusion index α by fitting the data of the last 10^4 kicks to Eq. (10). Part (a) is for $K = 1$. Part (b) is similar to (a), but for $K = 10$. Part (c) is for $T = 2.05\pi$.

For the standard kicked rotor, if the free evolution part in Eq. (6) can be neglected, i.e., $\frac{\hbar T}{2m} = 2k\pi$, then from Eqs. (21) and (22) it can be proved that

$$\psi_l(nT) = \frac{1}{\sqrt{2\pi}} e^{-ila_0} i^{-l} J_{-l}\left(-\frac{nK}{\hbar}\right) \tag{23}$$

and

$$\begin{aligned}\langle \Delta L_n^2 \rangle &= \langle L_n^2 - L_0^2 \rangle \\ &= \sum_l (\hbar l)^2 [|\psi_l(nT)|^2 - |\psi_l(0)|^2] \\ &= \frac{\hbar^2}{2\pi} \sum_l l^2 J_{-l}^2\left(-\frac{nK}{\hbar}\right) \\ &= \frac{\hbar^2}{4\pi}\left(\frac{nK}{\hbar}\right)^2 = \frac{K^2}{4\pi} n^2. \end{aligned} \tag{24}$$

Therefore, in this case, the expectation value of the rotor's energy grows ballistically ($\sim n^2$) for arbitrary n and K, which is denoted as quantum resonance [9,19,35–42]. On the contrary, if $\frac{\hbar T}{2m} = (2k+1)\pi$, then

$$\psi_l(nT) = \begin{cases} \frac{1}{\sqrt{2\pi}} \delta_{l,0} & \text{for even } n, \\ \frac{1}{\sqrt{2\pi}} e^{-ila_0} i^{-l} J_{-l}(\frac{K}{\hbar}) & \text{for odd } n. \end{cases} \tag{25}$$

In this case, we have

$$\langle \Delta L_n^2 \rangle = \begin{cases} 0 & \text{for even } n, \\ \frac{K^2}{4\pi} & \text{for odd } n, \end{cases} \tag{26}$$

and the expectation value of the rotor's energy will return to its initial value after every two kicks, which is denoted as quantum antiresonance [9,19,35,37–42].

As we can see from Figs. 7(a) and 7(b), if the resonance condition is met (e.g., $T = 4\pi$), then the diffusion index α will always be 2, irrespective of the value of K. On the contrary, if $\frac{\hbar T}{2m}$ is irrational to π (e.g., $T = 1.1$), then α will be 0 for arbitrary K, and this phenomenon is the well-known dynamical localization [34]. Finally, if the resonance condition is not met and $\frac{\hbar T}{2m}$ is rational to π [e.g., $T = 2.05\pi$ as shown in Fig. 7(c)], then depending on the values of T and K, the behavior of $\langle \Delta L_n^2 \rangle$ at large n can switch between ballistic diffusion ($\alpha = 2$) and localization ($\alpha = 0$). Throughout the parameter space of T and K, we did not find a diffusion index α other than 2 and 0, suggesting that in the standard kicked rotor, $\langle \Delta L_n^2 \rangle$ exhibits only ballistic diffusion or localization.

For the periodically shifted case with $a_n = \pi \cos(\frac{\pi}{2} n)$, since $a_{n+1} - a_n = \pm\pi$, it can be proved that the resonance condition of the standard kicked rotor now becomes the antiresonance one, and vice versa [5]. The behavior of $\langle \Delta L_n^2 \rangle$ is similar between these two cases, which shows only ballistic diffusion or localization, as can be seen from Figs. 8(a)–8(c). If we set $a_n = \frac{\pi}{6} \cos(\frac{\pi}{2} n)$, although the resonance condition cannot be satisfied, the conclusion is qualitatively similar to that of $a_n = \pi \cos(\frac{\pi}{2} n)$, as shown in Fig. 9.

For the other periodically shifted case with $\{a_0, a_1, a_2, a_3\}$ picked randomly from $-\pi$ to π, after averaging over various random number realizations, we have

$$\overline{|\psi_{l_n}(nT)|^2} = \frac{1}{(2\pi)^4} \int_{-\pi}^{\pi} da_0 \cdots \int_{-\pi}^{\pi} da_3 |\psi_{l_n}(nT)|^2. \tag{27}$$

Then by using the relation

$$\frac{1}{2\pi} \int_{-\pi}^{\pi} d\theta \, e^{i(l-l')\theta} = \delta_{l,l'}, \tag{28}$$

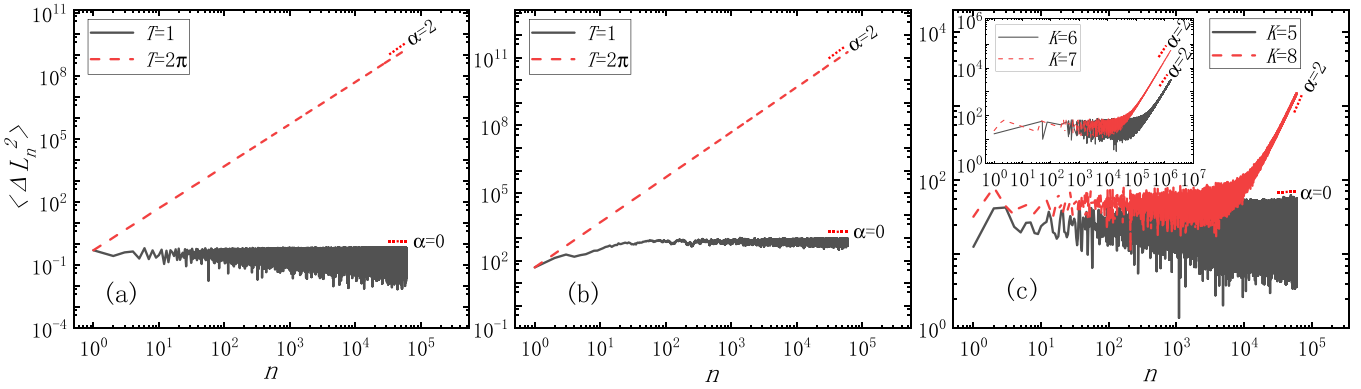

FIG. 8. Similar to Fig. 7, but for the periodically shifted case with $a_n = \pi \cos(\frac{\pi}{2}n)$. Part (a) is for $K = 1$. Part (b) is similar to (a), but for $K = 10$. Part (c) is for $T = 2.05\pi$.

and the properties of the Bessel function, it can be proved that, for $\frac{\hbar T}{2m} = k\pi$,

$$\begin{aligned}\langle \Delta L_n^2 \rangle &= \hbar^2 \sum_{l_n} l_n^2 \overline{|\psi_{l_n}(nT)|^2} \\ &= \begin{cases} \frac{K^2}{4\pi} n & \text{when } 1 \leqslant n \leqslant 4, \\ \frac{K^2}{16\pi} n^2 & \text{when } n > 4 \text{ and } \mathrm{mod}(n,4) = 0, \\ \frac{K^2}{16\pi}(n^2+3) & \text{when } n > 4 \text{ and } \mathrm{mod}(n,4) = 1 \text{ or } 3, \\ \frac{K^2}{16\pi}(n^2+4) & \text{when } n > 4 \text{ and } \mathrm{mod}(n,4) = 2. \end{cases}\end{aligned} \tag{29}$$

Since in this case the expectation value of the rotor's energy also grows ballistically ($\sim n^2$) at large n for arbitrary K, it is denoted as quantum resonance as well. Therefore, both the resonance and antiresonance conditions of the standard kicked rotor become the resonance one for this periodically shifted case. On the other hand, if $\frac{\hbar T}{2m}$ is irrational to π, then similar to the above two cases, $\langle \Delta L_n^2 \rangle$ will exhibit dynamical localization [see the $T = 1$ case in Figs. 10(a) and 10(b)]. On the contrary, if the resonance condition is not met and $\frac{\hbar T}{2m}$ is rational to π, then unlike the above two cases, $\langle \Delta L_n^2 \rangle$ will not show any localization-delocalization transition and exhibit only ballistic diffusion, irrespective of K [see the $T = \pi$ case in Figs. 10(a) and 10(b)]. Intuitively, it was suggested that the ballistic energy growth should stem from quantum interference, and random modulation should destroy it. However, here we show that, with random but periodic phase modulation, the quantum coherence is retained and the parameter space for observing ballistic energy diffusion is greatly enlarged. If $\{a_0, a_1, a_2, a_3\}$ is picked randomly from $-\frac{\pi}{6}$ to $\frac{\pi}{6}$, the conclusion is qualitatively similar to the above case, as shown in Fig. 11.

For the randomly shifted case, since each a_n is randomly picked from $-\pi$ to π, therefore, similar to Eqs. (27) and (28), we have

$$\begin{aligned}\overline{|\psi_{l_n}(nT)|^2} &= \frac{1}{(2\pi)^n} \int_{-\pi}^{\pi} da_0 \cdots \int_{-\pi}^{\pi} da_{n-1} |\psi_{l_n}(nT)|^2 \\ &= \frac{1}{2\pi} \sum_{l_1} \cdots \sum_{l_{n-1}} J^2_{l_{n-1}-l_n}\left(-\frac{K}{\hbar}\right) \cdots J^2_{l_1-l_2}\left(-\frac{K}{\hbar}\right) J^2_{-l_1}\left(-\frac{K}{\hbar}\right).\end{aligned} \tag{30}$$

Furthermore, by using the relation

$$\sum_{l_n} l_n^2 \sum_{l_1} \cdots \sum_{l_{n-1}} J^2_{l_{n-1}-l_n}\left(-\frac{K}{\hbar}\right) \cdots J^2_{l_1-l_2}\left(-\frac{K}{\hbar}\right) J^2_{-l_1}\left(-\frac{K}{\hbar}\right) = \frac{n}{2}\left(\frac{K}{\hbar}\right)^2, \tag{31}$$

we have

$$\langle \Delta L_n^2 \rangle = \frac{K^2}{4\pi} n, \tag{32}$$

which means that, in the randomly shifted case, the expectation value of the rotor's energy always shows normal diffusion ($\sim n$), as evidenced by Figs. 12(a) and 12(b). The reason is that the addition of random phase modulation completely destroys

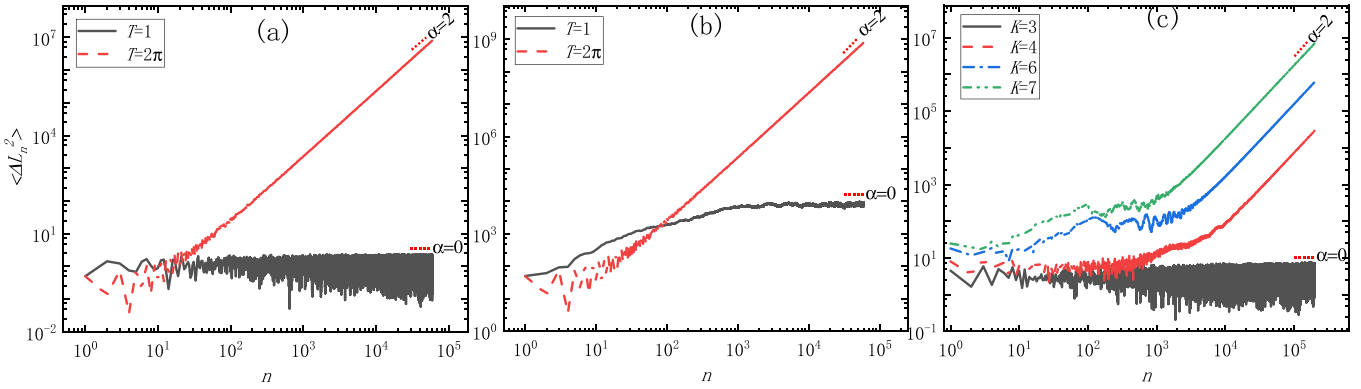

FIG. 9. Similar to Fig. 8, but for periodically shifted case with $a_n = \frac{\pi}{6}\cos(\frac{\pi}{2}n)$. Part (a) is for $K = 1$. Part (b) is similar to (a), but for $K = 10$. Part (c) is for $T = 2.05\pi$.

the quantum coherence and thus destroys the dynamical localization. Furthermore, the satisfaction of Eq. (30) destroys the quantum resonance. If each a_n is randomly picked from $-\frac{\pi}{6}$ to $\frac{\pi}{6}$, then Eq. (30) will not be satisfied. In this case, the dynamical localization should be destroyed while the quantum resonance should be retained. In Fig. 13 we can see that the expectation value of the rotor's energy still shows normal diffusion ($\sim n$) if $\frac{\hbar T}{2m}$ is not integer multiples of 2π (see the $T = 1$ and 2π cases). When $\frac{\hbar T}{2m}$ is integer multiples of 2π (see the $T = 4\pi$ case), which is the resonance condition of the standard model, $\langle \Delta L_n^2 \rangle$ shows ballistic diffusion ($\alpha = 2$), irrespective of the value of K.

Finally, for the quasiperiodically shifted case, the situation becomes more complicated. When $\frac{\hbar T}{2m} = 2k\pi$, then similar to the standard kicked case, $\langle \Delta L_n^2 \rangle$ shows resonance behavior and grows as n^2 for large n, irrespective of the value of K [see the $T = 4\pi$ case in Figs. 14(a) and 14(b)]. On the other hand, if $\frac{\hbar T}{2m} = (2k+1)\pi$, then $\langle \Delta L_n^2 \rangle$ will be localized for arbitrary K [see the $T = 2\pi$ case in Figs. 14(a) and 14(b)], similar to the antiresonance condition in the standard kicked case. Furthermore, if the above two conditions are not met while $\frac{\hbar T}{2m}$ is still rational to π [e.g., $T = 2.05\pi$ as shown in Fig. 14(c)], then depending on the values of T and K, the behavior of $\langle \Delta L_n^2 \rangle$ at large n can switch between ballistic diffusion ($\alpha = 2$) and localization ($\alpha = 0$), which is also similar to that in the standard kicked case. However, if $\frac{\hbar T}{2m}$ is irrational to π, then there will exist a critical value K_c, leading to $\alpha = 0$ for $K < K_c$ and $\alpha = 1$ for $K > K_c$ [e.g., the $T = 1$ case shown in Fig. 14(d)]. Besides, the value of K_c depends on the exact value of $\frac{\hbar T}{2m}$. Thus in this case, the behavior of $\langle \Delta L_n^2 \rangle$ can switch between normal diffusion ($\alpha = 1$) and localization ($\alpha = 0$). The above results indicate that the behaviors of ballistic diffusion, normal diffusion, as well as localization can all show up in the quasiperiodically shifted case. Therefore, it is somewhere between the standard kicked case and the randomly shifted one. And if we set $a_n = \frac{\pi}{6}\cos[\pi(\sqrt{5}-1)n]$, the conclusion is qualitatively similar to that of $a_n = \pi\cos[\pi(\sqrt{5}-1)n]$, as shown in Fig. 15.

In the above two cases, sequences produced by random modulation are nonrepeatable and need to be ensemble-averaged, which greatly increase the difficulty of experiment and calculation. However, the quasiperiodic sequence is similar to the random one in the degree of disorder, and is controllable and repeatable, therefore the previous work [5]

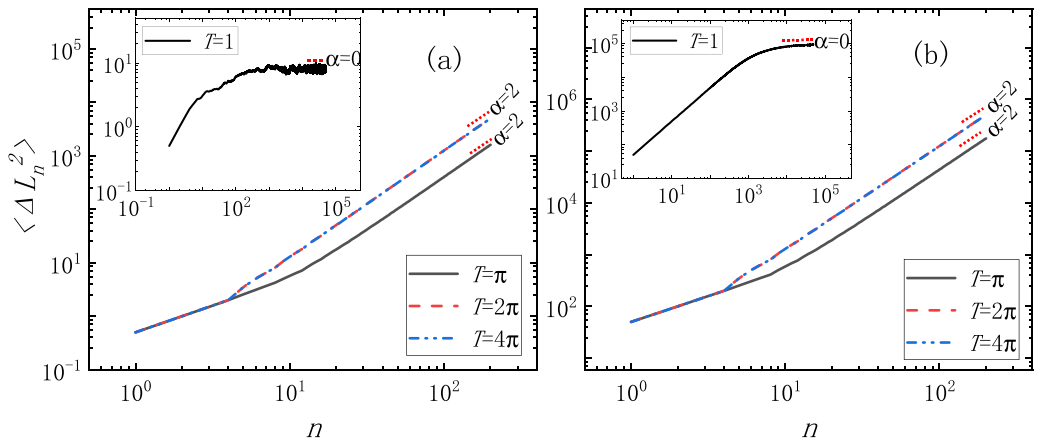

FIG. 10. Similar to Fig. 7, but for the periodically shifted case with $\{a_0, a_1, a_2, a_3\}$ picked randomly from $-\pi$ to π. Part (a) is for $K = 1$. Part (b) is similar to (a), but for $K = 10$.

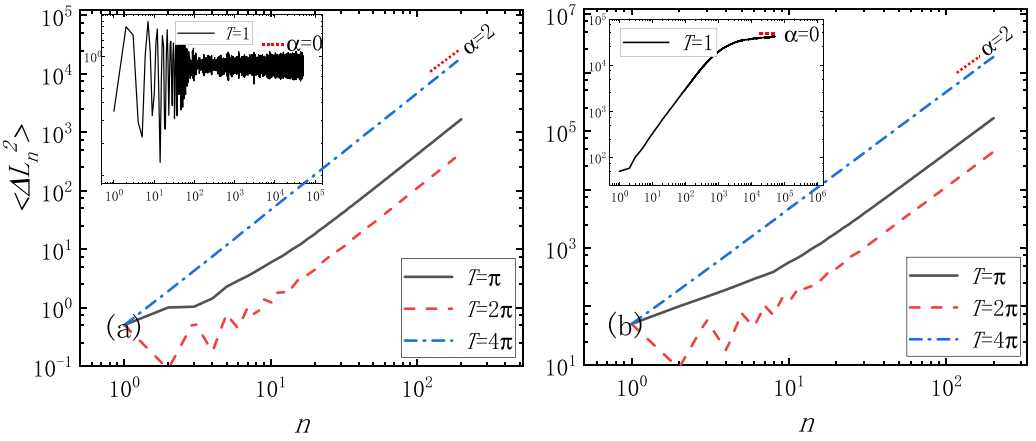

FIG. 11. Similar to Fig. 10, but for the periodically shifted case with $\{a_0, a_1, a_2, a_3\}$ picked randomly from $-\frac{\pi}{6}$ to $\frac{\pi}{6}$. Part (a) is for $K = 1$. Part (b) is similar to (a), but for $K = 10$.

suggested that quasiperiodic modulation can be regarded as representing a true white noise, which is a great convenience for experimental research. The relation between the white noise and incommensurate frequency can be understood from the Fourier treatment of Eq. (6) in Ref. [5]. When the number of kicks is sufficiently large, it becomes possible to resolve the incommensurate frequency in the Fourier spectrum. For a low number of kicks, the modulation has the approximate characteristics of white noise. For both the quantum resonance and dynamical localization, our results agree well with Ref. [5] in the presence of quasiperiodic phase modulation. An incommensurate frequency is equivalent to white noise at small n ($<10^2$) [5]. But at large n ($>10^3$), both our theoretical derivation and numerical simulation show that it is questionable to use the quasiperiodic phase modulation to represent the truly random one. In summary, we have theoretically investigated the effects of phase modulation on the classical and quantum kicked rotor [5]. By comparing the results, some unexpected discoveries are made. In the classical kicked rotor with phase modulation, due to the existence of acceleration island [33,43], anomalous diffusion is a common phenomenon as long as the phase a_n changes periodically and jumps by 0 or π from kick to kick. On the contrary, for random and quasiperiodic phase modulation, anomalous diffusion is suppressed, and the effect of the quasiperiodic phase modulation is inequivalent to the random one at large kicking times. For the quantum kicked rotor with phase modulation, in the standard and periodically shifted cases, it is worth noting that we did not find a diffusion index α other than 2 and 0, which indicates that there can exist only ballistic diffusion ($\alpha = 2$) or localization ($\alpha = 0$) in these cases [34]. Conversely, the addition of random phase modulation destroys the quantum coherence and totally suppresses the dynamical localization. Furthermore, the quasiperiodic phase modulation is an intermediate phase between the standard case and the random one.

ACKNOWLEDGMENTS

The authors would like to thank H. Fu for helpful discussion. We gratefully acknowledge the support of the National Natural Science Foundation of China (Grants No. 11975126 and No. 11874221).

APPENDIX A: THE DERIVATION OF EQS. (3)– (6)

The derivation of Eqs. (3)– (6) is as follows. We consider a kicked rotor whose Hamiltonian is given by

$$H(t) = \frac{L^2}{2m} + K\cos[\theta - a(t)]\sum_n \delta(t - nT), \tag{A1}$$

and the Schrödinger equation is

$$i\hbar\frac{\partial\Psi(\theta,t)}{\partial t} = H(t)\Psi(\theta,t). \tag{A2}$$

When the time t increases from $nT - 0^+$ to $nT + 0^+$, we have

$$\int_{\Psi(\theta,nT-0^+)}^{\Psi(\theta,nT+0^+)} \frac{1}{\Psi(\theta,t)} d\Psi(\theta,t) = -\frac{i}{\hbar}\int_{nT-0^+}^{nT+0^+} H(t)dt. \tag{A3}$$

Then

$$\ln\frac{\Psi(\theta,nT+0^+)}{\Psi(\theta,nT-0^+)} = -\frac{i}{\hbar}\int_{nT-0^+}^{nT+0^+} H(t)dt$$

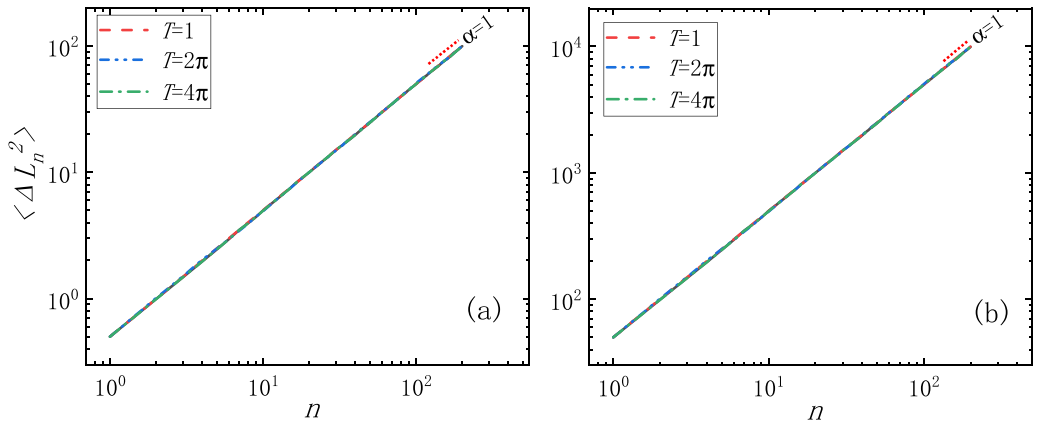

FIG. 12. Similar to Fig. 7, but for the randomly shifted case. Part (a) is for $K = 1$. Part (b) is similar to (a), but for $K = 10$.

$$= -\frac{i}{\hbar} K \cos[\theta - a(nT)]$$
$$= -\frac{i}{\hbar} K \cos(\theta - a_n). \tag{A4}$$

In the above, since the integral interval is infinitesimal, the contribution from the $\frac{L^2}{2m}$ term can be neglected on the right-hand side, and we use a_n to denote $a(nT)$, as mentioned right below Eq. (2). Therefore,

$$\Psi(\theta, nT + 0^+) = e^{-\frac{i}{\hbar} K \cos(\theta - a_n)} \Psi(\theta, nT - 0^+). \tag{A5}$$

Similarly, when the time t evolves from $nT + 0^+$ to $(n + 1)T - 0^+$, we have

$$\int_{\Psi(\theta, nT+0^+)}^{\Psi[\theta,(n+1)T-0^+]} \frac{1}{\Psi(\theta, t)} d\Psi(\theta, t) = -\frac{i}{\hbar} \int_{nT+0^+}^{(n+1)T-0^+} H(t) dt, \tag{A6}$$

and then

$$\ln \frac{\Psi[\theta, (n+1)T - 0^+]}{\Psi(\theta, nT + 0^+)} = -\frac{i}{\hbar} \int_{nT+0^+}^{(n+1)T-0^+} H(t) dt$$
$$= -\frac{i}{\hbar} \frac{L^2 T}{2m}. \tag{A7}$$

Therefore,

$$\Psi[\theta, (n+1)T - 0^+] = e^{-\frac{i}{\hbar} \frac{L^2 T}{2m}} \Psi(\theta, nT + 0^+)$$
$$= e^{-\frac{i}{\hbar} \frac{L^2 T}{2m}} e^{-\frac{i}{\hbar} K \cos(\theta - a_n)} \Psi(\theta, nT - 0^+). \tag{A8}$$

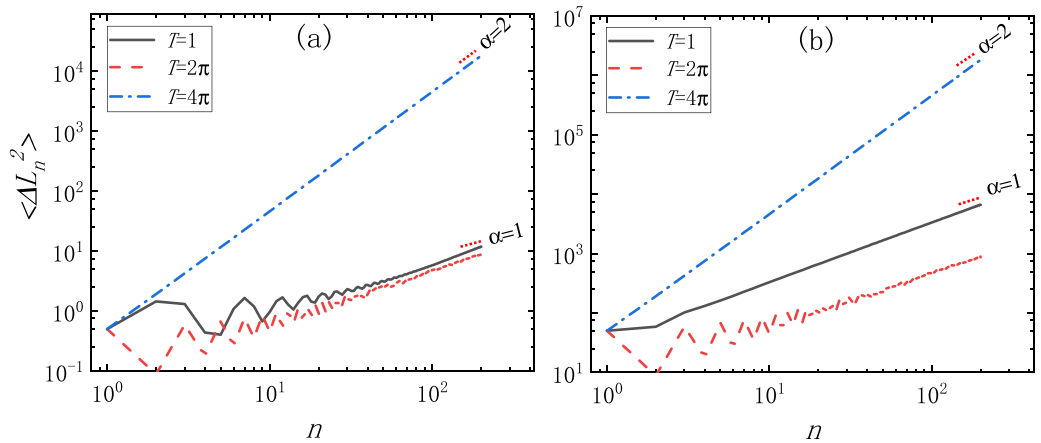

FIG. 13. Similar to Fig. 12, but for the randomly shifted case with each a_n randomly distributed from $-\frac{\pi}{6}$ to $\frac{\pi}{6}$. Part (a) is for $K = 1$. Part (b) is similar to (a), but for $K = 10$.

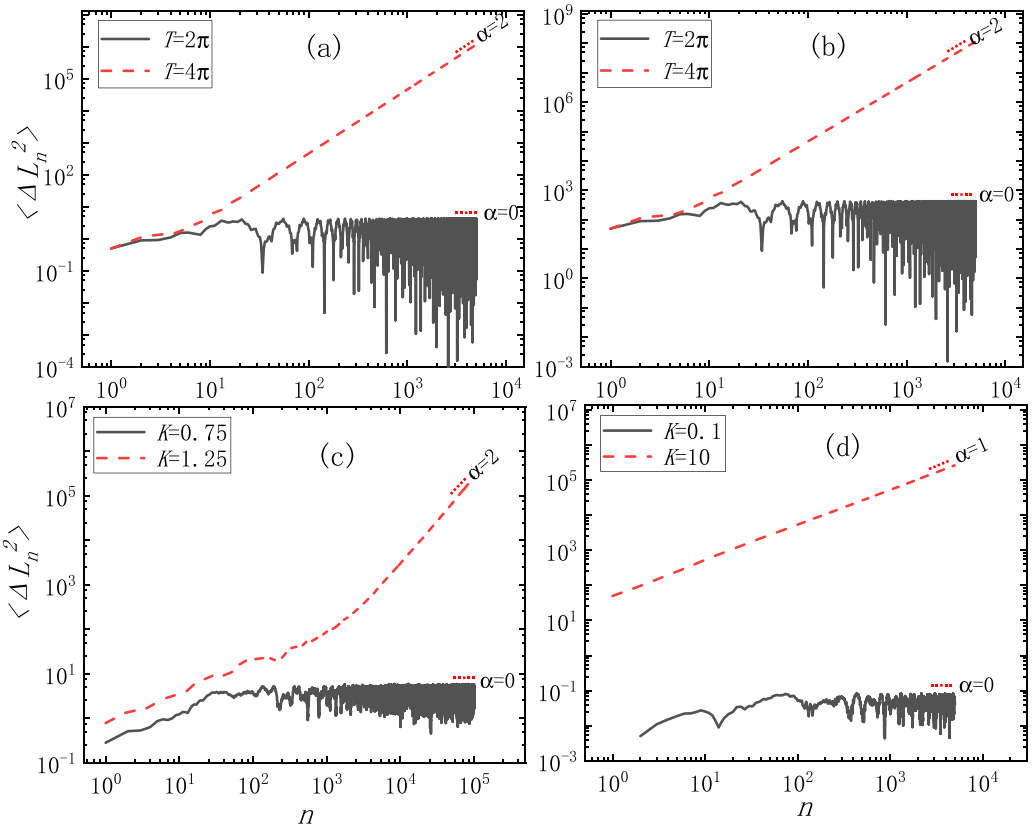

FIG. 14. Similar to Fig. 7, but for the quasiperiodically shifted case. Part (a) is for $K = 1$. Part (b) is similar to (a), but for $K = 10$. Part (c) is for $T = 2.05\pi$. Part (d) is similar to (c), but for $T = 1$.

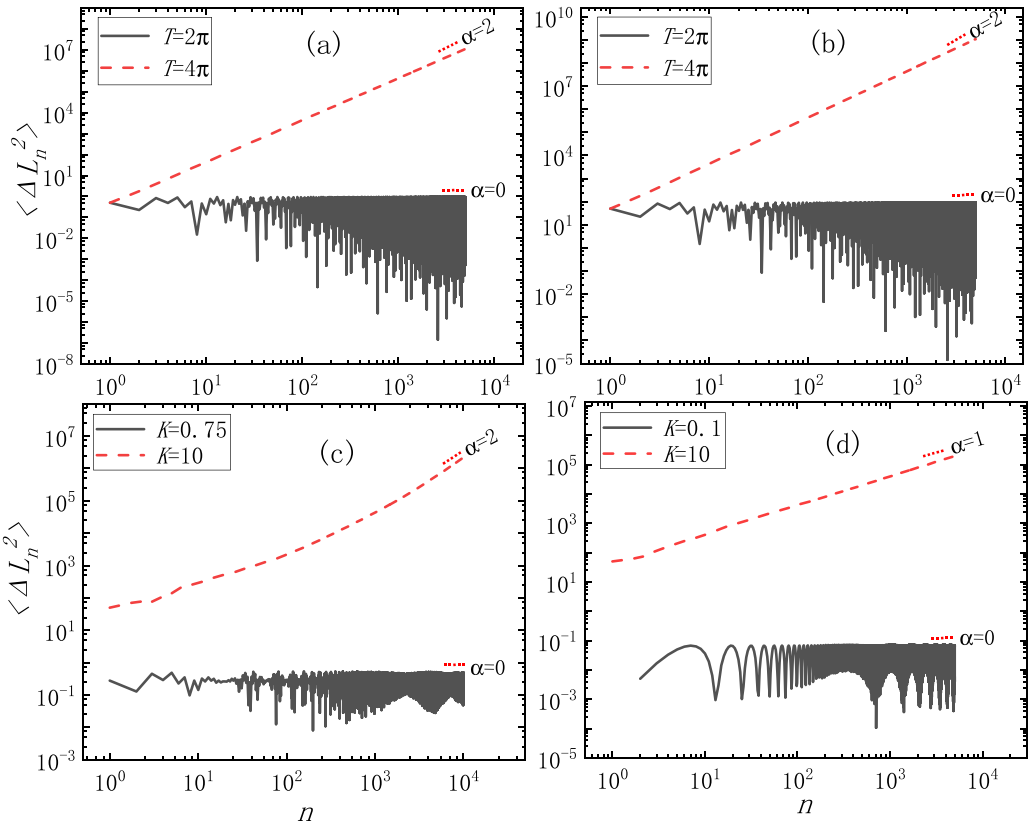

FIG. 15. Similar to Fig. 14, but for the quasiperiodically shifted case with $a_n = \frac{\pi}{6}\cos[\pi(\sqrt{5}-1)n]$. Part (a) is for $K = 1$. Part (b) is similar to (a), but for $K = 10$. Part (c) is for $T = 2.05\pi$. Part (d) is similar to (c), but for $T = 1$.

Thus, the time evolution operator over one period can be written as

$$U(n+1,n) = e^{-\frac{i}{\hbar}\frac{L^2T}{2m}} e^{-\frac{i}{\hbar}K\cos(\theta-a_n)}, \tag{A9}$$

which relates the wave functions at $t = nT$ and $t = (n+1)T$ as

$$\Psi[\theta, (n+1)T - 0^+] = U(n+1,n)\Psi(\theta, nT - 0^+). \tag{A10}$$

From the above, we can see that the time dependence of $a(t)$ has been considered through the a_n term in Eq. (A9). Furthermore, since the model is a δ-kicked one, only the value of $a(t)$ at $t = nT$ (i.e., a_n) matters, therefore Eqs. (3)– (5) are justified.

The wave function $\Psi(\theta, t)$ can be expressed by Fourier transform as $\Psi(\theta, t) = \sum_l e^{il\theta}\psi_l(t)$, and since $Le^{il\theta} = \hbar l e^{il\theta}$, we can take the Fourier transform of Eq. (A8),

$$\sum_{l'} e^{il'\theta}\psi_{l'}[(n+1)T - 0^+] = e^{-\frac{i}{\hbar}\frac{L^2T}{2m}} \sum_{l'} e^{il'\theta}\psi_{l'}(nT + 0^+), \tag{A11}$$

thus

$$\psi_{l'}[(n+1)T - 0^+] = e^{\frac{-il'^2\hbar T}{2m}}\psi_{l'}(nT + 0^+). \tag{A12}$$

Furthermore,

$$\begin{aligned}
\psi_{l'}(nT + 0^+) &= \frac{1}{2\pi}\int_0^{2\pi} e^{-il'\theta}\Psi(\theta, nT + 0^+)d\theta \\
&= \frac{1}{2\pi}\int_0^{2\pi} e^{-il'\theta}e^{-\frac{i}{\hbar}K\cos(\theta-a_n)}\Psi(\theta, nT - 0^+)d\theta \\
&= \frac{1}{2\pi}\int_0^{2\pi} e^{-il'\theta}e^{-\frac{i}{\hbar}K\cos(\theta-a_n)}\sum_l e^{il\theta}\psi_l(nT - 0^+)d\theta.
\end{aligned} \tag{A13}$$

Then by inserting Eq. (A13) into Eq. (A12), we have

$$\psi_{l'}[(n+1)T - 0^+] = \frac{1}{2\pi}e^{-\frac{il'^2\hbar T}{2m}}\int_0^{2\pi} e^{-il'\theta}e^{-\frac{i}{\hbar}K\cos(\theta-a_n)}\sum_l e^{il\theta}\psi_l(nT - 0^+)d\theta. \tag{A14}$$

By letting $\theta' = \theta - a_n$ and $\theta = \theta' + a_n$, we have

$$\psi_{l'}[(n+1)T - 0^+] = \frac{1}{2\pi}e^{-\frac{il'^2\hbar T}{2m}}\sum_l\int_0^{2\pi} e^{i(l-l')(\theta'+a_n)}e^{-\frac{i}{\hbar}K\cos\theta'}\psi_l(nT - 0^+)d\theta'. \tag{A15}$$

Then substituting θ' by θ,

$$\psi_{l'}[(n+1)T - 0^+] = \frac{1}{2\pi}e^{-\frac{il'^2\hbar T}{2m}}\sum_l\int_0^{2\pi} e^{i(l-l')\theta}e^{i(l-l')a_n}e^{-\frac{i}{\hbar}K\cos\theta}\psi_l(nT - 0^+)d\theta. \tag{A16}$$

The Bessel function is expressed as

$$J_{l-l'}\left(-\frac{K}{\hbar}\right) = \frac{1}{2\pi}i^{-(l-l')}\int_0^{2\pi} e^{i(l-l')\theta}e^{-\frac{i}{\hbar}K\cos\theta}d\theta, \tag{A17}$$

thus

$$\psi_{l'}[(n+1)T - 0^+] = e^{-\frac{il'^2\hbar T}{2m}}\sum_l J_{l-l'}\left(-\frac{K}{\hbar}\right)e^{i(l-l')a_n}i^{l-l'}\psi_l(nT - 0^+). \tag{A18}$$

This is Eq. (6), and the time dependence of $a(t)$ is also considered as a_n.

APPENDIX B: THE DERIVATION OF EQS. (11)–(13)

For the classical kicked rotor, the dynamics of the system can be described by the standard map,

$$\begin{aligned}
L_{n+1} &= L_n + K\sin(\theta_n - a_n), \\
\theta_{n+1} &= \theta_n + \frac{T}{m}L_{n+1}.
\end{aligned} \tag{B1}$$

For the standard kicked rotor, if the initial angular momentum L_0 and the initial angular position θ_0 satisfy

$$\begin{aligned}
\frac{T}{m}L_0 &= 2k\pi, \\
\frac{T}{m}K\sin(\theta_0 - a_0) &= 2l\pi,
\end{aligned} \tag{B2}$$

then we can multiply both sides of Eq. (B2) by $\frac{m}{T}$, and we will obtain

$$L_0 = \frac{\pi m}{T} 2k,$$
$$K \sin(\theta_0 - a_0) = \frac{\pi m}{T} 2l. \tag{B3}$$

For the standard kicked rotor, the phase a_n is constant (i.e., $a_0 = a_1 = a_2 = \cdots$). According to the initial conditions Eq. (B3) and the standard map Eq. (B1), we can get the angular momentum L_1 and the angular position θ_1 after one kick,

$$\begin{aligned} L_1 &= L_0 + K \sin(\theta_0 - a_0) \\ &= \frac{\pi m}{T} 2k + \frac{\pi m}{T} 2l \\ &= \frac{\pi m}{T}(2k + 2l), \\ \theta_1 &= \theta_0 + \frac{T}{m} L_1 \\ &= \theta_0 + \frac{T}{m}\frac{\pi m}{T}(2k + 2l) \\ &= \theta_0 + \pi(2k + 2l). \end{aligned} \tag{B4}$$

Then the angular momentum L_2 and the angular position θ_2 after two kicks are

$$\begin{aligned} L_2 &= L_1 + K \sin(\theta_1 - a_0) \\ &= \frac{\pi m}{T}(2k + 2l \times 2), \\ \theta_2 &= \theta_1 + \frac{T}{m} L_2 \\ &= \theta_0 + \pi(2k \times 2 + 2l \times 3). \end{aligned} \tag{B5}$$

Similarly, the angular momentum L_3 and the angular position θ_3 after three kicks can be obtained as

$$\begin{aligned} L_3 &= L_2 + K \sin(\theta_2 - a_0) \\ &= \frac{\pi m}{T}(2k + 2l \times 3), \\ \theta_3 &= \theta_2 + \frac{T}{m} L_3 \\ &= \theta_0 + \pi(2k \times 3 + 2l \times 6). \end{aligned} \tag{B6}$$

The angular momentum L_4 and the angular position θ_4 after four kicks are

$$\begin{aligned} L_4 &= L_3 + K \sin(\theta_3 - a_0) \\ &= \frac{\pi m}{T}(2k + 2l \times 4), \\ \theta_4 &= \theta_3 + \frac{T}{m} L_4 \\ &= \theta_0 + \pi(2k \times 4 + 2l \times 10). \end{aligned} \tag{B7}$$

The angular momentum L_5 and the angular position θ_5 after five kicks are

$$\begin{aligned} L_5 &= L_4 + K \sin(\theta_4 - a_0) \\ &= \frac{\pi m}{T}(2k + 2l \times 5), \\ \theta_5 &= \theta_4 + \frac{T}{m} L_5 \\ &= \theta_0 + \pi(2k \times 5 + 2l \times 15), \end{aligned} \tag{B8}$$

$$\cdots \quad \cdots$$

By mathematical induction, we can get the angular momentum L_n and the angular position θ_n after n kicks as

$$\begin{aligned} L_n &= \frac{\pi m}{T}(2k + 2l \times n), \\ \theta_n &= \theta_0 + [2k \times n + n(n+1)l]\pi. \end{aligned} \tag{B9}$$

The initial angular momentum L_0 is

$$L_0 = \frac{\pi m}{T} 2k. \tag{B10}$$

Therefore, by substituting Eq. (B10) into Eq. (B9), the relation between L_n and L_0 can be obtained, which is

$$L_n = L_0 + \frac{\pi m}{T} 2ln. \tag{B11}$$

Now we get the rotor's energy growth ΔL_n^2 with the initial angular momentum L_0 and the initial angular position θ_0 satisfying Eq. (B3), which is

$$\begin{aligned} \Delta L_n^2 &= L_n^2 - L_0^2 \\ &= \left(L_0 + \frac{\pi m}{T} 2ln\right)^2 - L_0^2 \\ &= \frac{\pi m}{T} 2l \left[\frac{\pi m}{T} 2ln^2 + 2L_0 n\right]. \end{aligned} \tag{B12}$$

And according to Eq. (B3), we know that

$$\frac{\pi m}{T} 2l = K \sin(\theta_0 - a_0). \tag{B13}$$

With Eq. (B13) substituted into Eq. (B12), we can get the rotor's energy growth ΔL_n^2 after n kicks as

$$\Delta L_n^2 = K \sin(\theta_0 - a_0)[K \sin(\theta_0 - a_0) n^2 + 2L_0 n]. \tag{B14}$$

This leads to Eq. (13), and from Eq. (B9) we know that θ_n and θ_0 differ only by integer multiples of 2π. Together with $a_0 = a_1 = a_2 = \cdots$, hence the following relation should hold:

$$K \sin(\theta_0 - a_0) = K \sin(\theta_1 - a_1) = \cdots K \sin(\theta_n - a_n). \tag{B15}$$

[1] W. H. Zurek, Decoherence, einselection, and the quantum origins of the classical, Rev. Mod. Phys. **75**, 715 (2003).

[2] M. I. Dykman, H. Rabitz, V. N. Smelyanskiy, and B. E. Vugmeister, Resonant Directed Diffusion in Nonadiabatically Driven Systems, Phys. Rev. Lett. **79**, 1178 (1997).

[3] I. Walmsley and H. Rabitz, Quantum physics under control, Phys. Today **56**, 43 (2003).

[4] M. Sadgrove, T. Schell, K. Nakagawa, and S. Wimberger, Engineering quantum correlations to enhance transport in cold atoms, Phys. Rev. A **87**, 013631 (2013).

[5] D. H. White, S. K. Ruddell, and M. D. Hoogerland, Phase noise in the delta kicked rotor: From quantum to classical, New J. Phys. **16**, 113039 (2014).

[6] G. Casati and J. Ford, Stochastic behavior in classical and quantum Hamiltonian systems, Lect. Notes Phys. **93**, 334 (1979).

[7] B. V. Chirikov, F. M. Izrailev, and D. L. Shepelyansky, Dynamical stochasticity in classical and quantum mechanics, Sov. Scient. Rev. (Gordon and Bridge) **2C**, 209 (1981).

[8] E. Ott, T. M. Antonsen, and J. D. Hanson, Effect of Noise on Time-Dependent Quantum Chaos, Phys. Rev. Lett. **53**, 2187 (1984).

[9] M. Sadgrove, A. Hilliard, T. Mullins, S. Parkins, and R. Leonhardt, Observation of robust quantum resonance peaks in an atom optics kicked rotor with amplitude noise, Phys. Rev. E **70**, 036217 (2004).

[10] D. Cohen, Quantum chaos, dynamical correlations, and the effect of noise on localization, Phys. Rev. A **44**, 2292 (1991).

[11] M. B. d'Arcy, R. M. Godun, M. K. Oberthaler, D. Cassettari, and G. S. Summy, Quantum Enhancement of Momentum Diffusion in the Delta-Kicked Rotor, Phys. Rev. Lett. **87**, 074102 (2001).

[12] M. Sadgrove, T. Mullins, S. Parkins, and R. Leonhardt, The effect of amplitude noise on the quantum and diffusion resonances of the atom optics kicked rotor, J. Phys. E **29**, 369 (2005).

[13] M. Lepers, V. Zehnlé, and J. C. Garreau, Suppression of decoherence-induced diffusion in the quantum kicked rotor, Phys. Rev. A **81**, 062132 (2010).

[14] J. C. Garreau, Quantum simulation of disordered systems with cold atoms, C. R. Phys. **18**, 31 (2017).

[15] D. H. White, S. K. Ruddell, and M. D. Hoogerland, Experimental realization of a quantum ratchet through phase modulation, Phys. Rev. A **88**, 063603 (2013).

[16] F. L. Moore, J. C. Robinson, C. F. Bharucha, B. Sundaram, and M. G. Raizen, Atom Optics Realization of the Quantum δ-Kicked Rotor, Phys. Rev. Lett. **75**, 4598 (1995).

[17] C. F. Bharucha, J. C. Robinson, F. L. Moore, B. Sundaram, Q. Niu, and M. G. Raizen, Dynamical localization of ultracold sodium atoms, Phys. Rev. E **60**, 3881 (1999).

[18] H. Ammann, R. Gray, I. Shvarchuck and N. Christensen, Quantum Delta-Kicked Rotor: Experimental Observation of Decoherence, Phys. Rev. Lett. **80**, 4111 (1998).

[19] W. H. Oskay, D. A. Steck, V. Milner, B. G. Klappauf, and M. G. Raizen, Ballistic peaks at quantum resonance, Opt. Commun. **179**, 137 (2000).

[20] D. A. Steck, V. Milner, W. H. Oskay, and M. G. Raizen, Quantitative study of amplitude noise effects on dynamical localization, Phys. Rev. E **62**, 3461 (2000).

[21] A. J. Daley, Action space diffusion resonances for an atom optics kicked rotor with decoherence and amplitude noise, M.Sc. thesis, University of Auckland (2002).

[22] J. Chabé, G. Lemarié, B. Grémaud, D. Delande, P. Szriftgiser, and J. C. Garreau, Experimental Observation of the Anderson Metal-Insulator Transition with Atomic Matter Waves, Phys. Rev. Lett. **101**, 255702 (2008).

[23] S. A. Wayper, W. Simpson, and M. D. Hoogerland, Short-time energies in the atom optics kicked rotor, Europhys. Lett. **79**, 60006 (2007).

[24] M. Bitter and V. Milner, Experimental Observation of Dynamical Localization in Laser-Kicked Molecular Rotors, Phys. Rev. Lett. **117**, 144104 (2016).

[25] H. Ammann, R. Gray, N. Christensen, and I. Shvarchuck, Experimental observation of dynamical localization and decoherence in the atomic δ-kicked rotor, J. Phys. B **31**, 2449 (1998).

[26] M. K. Oberthaler, R. M. Godun, M. B. d'Arcy, G. S. Summy, and K. Burnett, Observation of Quantum Accelerator Modes, Phys. Rev. Lett. **83**, 4447 (1999).

[27] R. Graham and S. Miyazaki, Dynamical localization of atomic de Broglie waves: The influence of spontaneous emission, Phys. Rev. A **53**, 2683 (1996).

[28] S. Dyrting, Modifications to the chaotic dynamics of laser-cooled atoms due to spontaneous emission, Phys. Rev. A **53**, 2522 (1996).

[29] C. Hainaut, P. Fang, A. Rancon, J.-F. Clément, P. Szriftgiser, J.-C. Garreau, C. Tian, and R. Chicireanu, Experimental Observation of a Time-Driven Phase Transition in Quantum Chaos, Phys. Rev. Lett. **121**, 134101 (2018).

[30] C. Hainaut, I. Manai, J.-F. Clément, J. C. Garreau, P. Szriftgiser, G. Lemarié, N. Cherroret, D. Delande, and R. Chicireanu, Controlling symmetry and localization with an artificial gauge field in a disordered quantum system, Nat. Commun. **9**, 1382 (2018).

[31] W.-L. Zhao, J. Gong, W.-G. Wang, G. Casati, J. Liu, and L.-B. Fu, Exponential wave-packet spreading via self-interaction time modulation, Phys. Rev. A **94**, 053631 (2016).

[32] D. R. Grempel, R. E. Prange, and S. Fishman, Quantum dynamics of a nonintegrable system, Phys. Rev. A **29**, 1639 (1984).

[33] Y. Zheng and D. H. Kobe, Anomalous momentum diffusion in the classical kicked rotor, Chaos Solitons Fractals **28**, 395 (2006).

[34] Y. Zheng and D. H. Kobe, Momentum diffusion of the quantum kicked rotor: Comparison of Bohmian and standard quantum mechanics, Chaos Solitons Fractals **34**, 1105 (2007).

[35] M. Bienert, F. Haug, W. P. Schleich, and M. G. Raizen, Kicked rotor in Wigner phase space, Fortschr. Phys. **51**, 474 (2003).

[36] F. M. Izrailev and D. L. Shepelyanskii, Quantum resonance for a rotator in a nonlinear periodic field, Theor. Math. Phys. **43**, 553 (1980).

[37] G. J. Duffy, S. Parkins, T. Müller, M. Sadgrove, R. Leonhardt, and A. C. Wilson, Experimental investigation of early-time diffusion in the quantum kicked rotor using a Bose-Einstein condensate, Phys. Rev. E **70**, 056206 (2004).

[38] A. J. Daley and A. S. Parkins, Early time diffusion for the quantum kicked rotor with narrow initial momentum distributions, Phys. Rev. E **66**, 056210 (2002).

[39] F. M. Izrailev and D. L. Shepelyansky, Quantum resonance for the rotor in a nonlinear periodic field, Dokl. Akad. Nauk SSSR **249**, 1103 (1979) [Sov. Phys. Dokl. **24**, 996 (1979)].

[40] G. Casati and I. Guarneri, Non-recurrent behaviour in quantum dynamics, Commun. Math. Phys. **95**, 121 (1984).

[41] V. V. Sokolov, O. V. Zhirov, D. Alonso, and G. Casati, Quantum Resonances of the Kicked Rotor and the SU(q) Group, Phys. Rev. Lett. **84**, 3566 (2000).

[42] C. Tian and A. Altland, Theory of localization and resonance phenomena in the quantum kicked rotor, New J. Phys. **12**, 043043 (2010).

[43] G. M. Zaslavsky, M. Edelman, and B. A. Niyazov, Self-similarity, renormalization, and phase space nonuniformity of Hamiltonian chaotic dynamics, Chaos **7**, 159 (1997).